



Cite this: DOI: 10.1039/c9cc09752j

 Received 16th December 2019,  
Accepted 21st January 2020

DOI: 10.1039/c9cc09752j

rsc.li/chemcomm

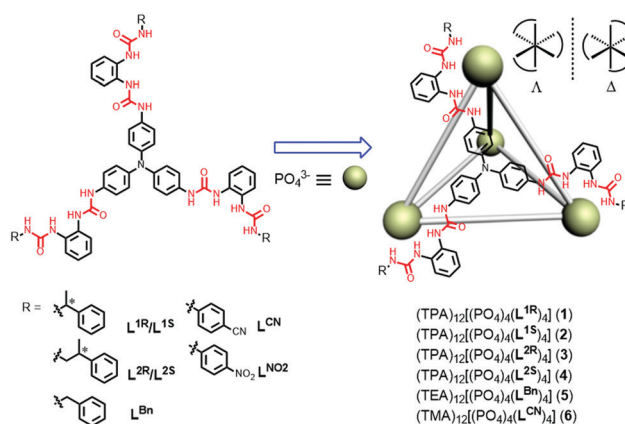
# Chirality transcription in the anion-coordination-driven assembly of tetrahedral cages†

 Jin Fu,<sup>‡</sup> Bo Zheng,<sup>‡</sup> Huizheng Zhang,<sup>a</sup> Yanxia Zhao,<sup>a</sup> Dan Zhang,<sup>a</sup>  
Wenyao Zhang,<sup>a</sup> Xiao-Juan Yang<sup>‡</sup> and Biao Wu<sup>‡\*ab</sup>

**Enantiopure  $A_4L_4$  tetrahedral cages (either  $\Delta\Delta\Delta\Delta$  or  $\Lambda\Lambda\Lambda\Lambda$ ) were obtained through the anion-coordination-driven assembly (ACDA) of phosphate anions with  $C_3$ -symmetric tris-bis(urea) ligands bearing chiral groups.**

The importance of chirality is underscored by its omnipresence in nature and significant practical applications.<sup>1</sup> To mimic biological systems, chemists have been studying the mechanism of chiral information transfer through the intricate interplay of non-covalent interactions in dynamic artificial systems.<sup>2</sup> In particular, great efforts have been devoted to develop well-organized, chiral discrete molecular cages or containers (MCs) through metal coordination, dynamic covalent chemistry (DCC), hydrogen bonding, *etc.*<sup>3</sup> Tetrahedral cages, the simplest Platonic solids, are one of the most extensively studied cage structures. The introduction of chirality into metal-coordination-based tetrahedral cages, both  $M_4L_4$  and  $M_4L_6$  ( $M$  = metal,  $L$  = ligand) types, has endowed these assemblies with useful potential in stereo-selective recognition and sensing, enantiomer separation, nonlinear optical materials, supramolecular asymmetric catalysis, *etc.*<sup>4</sup>

The anion-coordination-driven assembly (ACDA) as a new strategy has developed rapidly in recent years and exhibited high efficiency in the fabrication of organized, metal-free anion-supramolecular assemblies with fascinating properties.<sup>5</sup> In 2013, we reported the first tetrahedral anion  $A_4L_4$  cage ( $A$  = anion,  $L$  = ligand) assembled by a triphenylamine-based *o*-phenylene-bis(urea) ligand ( $L^{NO_2}$  in Scheme 1) and a phosphate anion.<sup>6</sup> Later, we replaced the triphenylamine core of the  $C_3$ -symmetric



**Scheme 1** Design of tris-bis(urea) ligands and the targeting  $A_4L_4$  chiral anion-supramolecular tetrahedral cages assembled by  $L$  and  $PO_4^{3-}$  in the presence of tetraalkylammonium cations.

tris-bis(urea) ligand with the triphenylbenzene and triphenyl-triazine units, respectively, and obtained the  $A_4L_4$  tetrahedral cages with larger cavities for guest inclusion.<sup>7</sup> These works illustrate a reliable and predictable way to build anion-cages based on  $C_3$ -symmetric ligands. Although each individual anion-tetrahedral cage is intrinsically chiral with either a  $\Delta\Delta\Delta\Delta$  or  $\Lambda\Lambda\Lambda\Lambda$  configuration at the four vertices (as octahedral complexes when taking one urea group as a coordinate vector), the whole complexes with the achiral ligands are always present as a racemic mixture.

In general, it is still challenging to control the chirality of the resultant assemblies by chiral auxiliaries in a predictable manner and without losing any chiral information.<sup>3e</sup> Recently, we set to explore the chiral resolution in the hydrogen-bonded anion-supramolecular assemblies, which might be more unpredictable than that in the metal-coordination systems. In the triple helicate system, chiral guests led to enantiopure structures capable of chirality sensing biomolecules.<sup>8</sup> However, by introducing chiral groups (which is a common way to realize chirality resolution in the assembled systems) into  $C_2$ -symmetric bis-bis(urea) ligands

<sup>a</sup> Key Laboratory of Synthetic and Natural Functional Molecule Chemistry of the Ministry of Education, College of Chemistry and Materials Science, Northwest University, Xi'an 710127, China. E-mail: wubiao@nwu.edu.cn

<sup>b</sup> State Key Laboratory of Applied Organic Chemistry, Lanzhou University, Lanzhou 730000, China

† Electronic supplementary information (ESI) available: Synthetic procedures, characterization data and corresponding CIF files. CCDC 1955042, 1955280 and 1957114. For ESI and crystallographic data in CIF or other electronic format see DOI: 10.1039/c9cc09752j

‡ These authors contributed equally to this work.

to build the  $A_4L_6$  tetrahedral cage or  $A_2L_3$  triple helicate, the expected assemblies were not obtained despite only small changes in the ligand.<sup>9</sup> So, we turned to the  $C_3$ -symmetric ligands which are more reliable for tetrahedral cages ( $A_4L_4$ -type). Two sets of ligands ( $L^{1R}/L^{1S}$  and  $L^{2R}/L^{2S}$ ; Scheme 1) were synthesized, which bear a similar point chirality on different positions (see details in the ESI†).<sup>6</sup> Notably, chirality transfer only occurred when the chiral carbon centers were directly attached to the urea groups ( $L^{1R}/L^{1S}$ ), while achiral cages were obtained when the chiral sites were one carbon away from the urea groups ( $L^{2R}/L^{2S}$ ). For comparison, ligand  $L^{Bn}$  (benzyl) without any chiral center was also prepared, as an achiral analogue of  $L^{1R/1S}$ .

Treatment of ligand  $L^{1R}$  or  $L^{1S}$  (which as a free ligand is insoluble in acetone or acetonitrile) with an equimolar  $PO_4^{3-}$  anion (as tetraalkylammonium salts) in acetonitrile eventually gave a clear solution. X-ray-quality crystals of two anion complexes (1 and 2) were successfully obtained by slow vapor diffusion of diethyl ether into their acetonitrile solutions. As expected, ligands  $L^{1R}$  and  $L^{1S}$  self-assemble with phosphate to form  $A_4L_4$ -type aniono tetrahedral cages,  $(TPA)_{12}[(PO_4)_4(L^{1R})_4]$  (1) and  $(TPA)_{12}[(PO_4)_4(L^{1S})_4]$  (2), respectively, with phosphate ions as four vertices and ligands as the faces (Fig. 1). Besides, the single crystals of the tetrahedral cage  $(TEA)_{12}[(PO_4)_4(L^{Bn})_4]$  (5) (TEA = tetraethylammonium) were isolated in the same way from the achiral ligand  $L^{Bn}$  (Fig. S44, ESI†). The noncovalent interactions in these structures are similar to previously reported  $A_4L_4$  aniono-cages<sup>6</sup> with twelve N-H...O hydrogen bonds between six urea groups and a phosphate center at each vertex. The hydrogen bond parameters are very close in the two enantiomers 1 and 2, with N...O distances ranging from 2.70 to 3.03 Å and N-H...O angles from 135° to 179° (Tables S1 and S2, ESI†). The cages of both achiral ligands  $L^{NO2}$  and  $L^{Bn}$  have quite uniform  $PO_4 \cdots PO_4$  separations,<sup>6</sup> at about 15 Å and the N...N (triphenylamine) separation between every two ligands is 7.12 Å. However, the tetrahedral cavity formed by the chiral ligands  $L^{1R/1S}$  is distorted, stretching in one direction (Fig. 1a), where the  $PO_4 \cdots PO_4$  separations range from about 13.6 to 15.3 Å, and N...N separations from 5.84 to 6.56 Å. Besides, the distribution of the three bis(urea) groups around a phosphate ion in the enantiopure chiral cages is less symmetric than that from the achiral ligands, displaying a twisted fashion due to the steric hindrance. Two of them lie horizontally and the remaining one reaches out, on top of the phosphate (Fig. 1c). TPA cations in the crystal structure are found outside the cage and all of them are located very close to the tetrahedron, either in the grooves formed by adjacent ligands or around the vertices (Fig. S45, ESI†).

Complexes 1 and 2 are present as mirror images, both in the chiral space group  $C_2$ . Cage 1 (with  $L^{1R}$ ) contains solely a  $\Delta\Delta\Delta\Delta$  configuration for all four vertices, while cage 2 (with  $L^{1S}$ ) shows a single  $\Lambda\Lambda\Lambda\Lambda$  configuration. In contrast, the tetrahedral cages constructed from the achiral ligands  $L^{NO2}$  and  $L^{Bn}$  (Fig. S44, ESI†) crystallize in the space group  $P\bar{4}_2c$ , with both  $\Delta\Delta\Delta\Delta$  and  $\Lambda\Lambda\Lambda\Lambda$  tetrahedra in the same unit cell as a racemic mixture. Thus, it appears that the chiral auxiliaries in the individual ligand have defined the consequent chiral structure.

To further investigate the impact of the chiral auxiliary, we studied the assembly of the ligand pair  $L^{2R}/L^{2S}$ . Treatment of

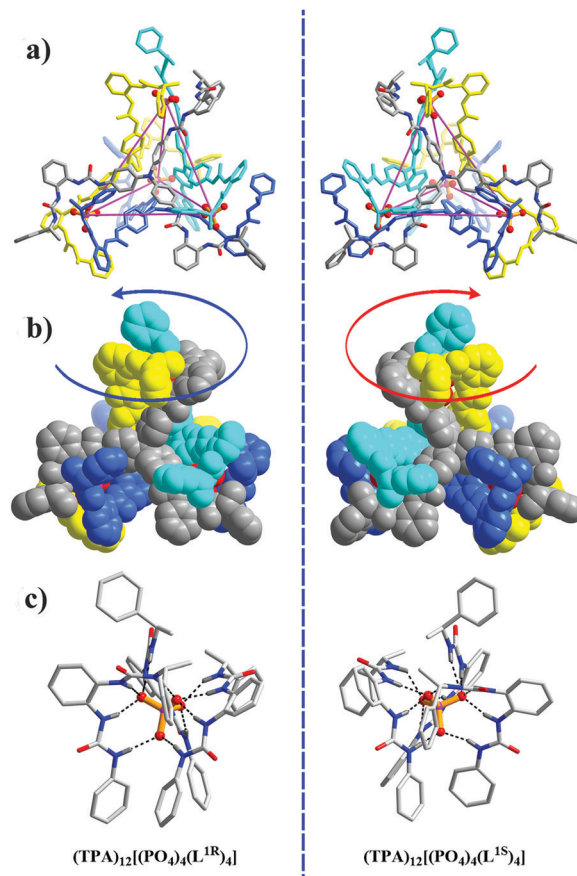


Fig. 1 Crystal structures of the homochiral cages 1  $[(PO_4)_4(L^{1R})_4]^{12-}$  ( $\Delta\Delta\Delta\Delta$ ) and 2  $[(PO_4)_4(L^{1S})_4]^{12-}$  ( $\Lambda\Lambda\Lambda\Lambda$ ). (a) View from the triangular face; (b) space-filling representation; and (c) hydrogen bonds formed between a  $PO_4^{3-}$  ion and six urea (three bis-urea) units. TPA<sup>+</sup> cations are omitted for clarity.

$L^{2R}/L^{2S}$  with an equimolar  $PO_4^{3-}$  anion (as tetraalkylammonium salts) afforded complexes 3 and 4. Unfortunately, despite many attempts with different crystallization methods, we were unable to get X-ray-quality single crystals of them. Therefore, several characterization methods were employed to investigate the two complexes in solution, which indicate that complexes 3 and 4 in solution exist as diastereomers (*vide infra*).

The  $^1H$  NMR spectrum of complex 1 (in acetone- $d_6$ ) reveals significant downfield shifts ( $\Delta\delta$  from 1.10 to 3.16 ppm) of the urea NH hydrogen signals compared to those of  $L^{1R}$  (NMR spectra of ligands used here were measured in DMSO- $d_6$  for solubility reasons) (Fig. 2 and Fig. S26 and S27, ESI†). According to previous studies, these shifts are caused by the typical coordination between phosphate anions and urea moieties and are in line with the results of the previously reported aniono-cages.<sup>6,7</sup> The protons in the aromatic region, H4, H5, H9 and H11, shift to upfield due to the shielding effect of the closely packed anion complex, while H2, H3 and H6 suffer downfield shifts caused by the anion-urea bonding. Besides, it should be noted that the NH hydrogens on urea groups split into two sets of peaks, indicating the formation of a low-symmetrical structure, which is consistent with the twisting distribution of the ligands at each vertex in the crystal structure.

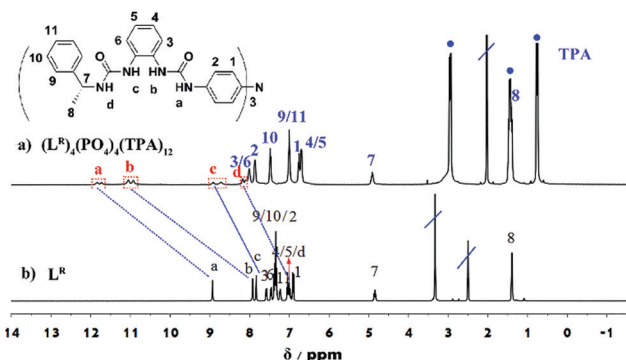


Fig. 2  $^1\text{H}$  NMR spectra (400 MHz, 298 K) of (a)  $(\text{TPA})_{12}[(\text{PO}_4)_4(\text{L}^{1\text{R}})_4]$  in acetone- $d_6$  and (b) ligand  $\text{L}^{1\text{R}}$  in  $\text{DMSO}-d_6$ . Signals of  $\text{TPA}^+$  are labelled by ● and solvent residues by /.

In contrast, the peaks of NH hydrogens in the NMR spectrum of the achiral ( $\text{L}^{\text{Bn}}$ ) complex 5 show only one set of signals, indicating the formation of a more symmetric coordinate geometry in solution (Fig. S31, ESI $^\dagger$ ) compared with the distorted distribution in  $\text{L}^{1\text{R}}/\text{L}^{1\text{S}}$ . This is probably ascribed to the removal of the chiral centre (a methyl substituent) to release steric hindrance for  $\text{L}^{\text{Bn}}$  compared with  $\text{L}^{1\text{R}}$ . The same complexation behavior between the phosphate ion and the urea moieties was also observed in complex 2, which means that both  $\text{L}^{1\text{R}}$  and  $\text{L}^{1\text{S}}$  ligands self-assembled with the anions into a similar structure.

$^1\text{H}$  NMR experiments were also performed to characterize the assemblies formed by  $\text{L}^{2\text{R}}$  and  $\text{L}^{2\text{S}}$  (Fig. S28 and S29, ESI $^\dagger$ ). Similarly, urea hydrogens of  $\text{L}^{2\text{S}}$  suffer significant downfield shifts as those of  $\text{L}^{1\text{R}}$  and  $\text{L}^{1\text{S}}$  (Fig. S30, ESI $^\dagger$ ). Differently, there is only one set of NMR signals in the spectrum and the urea peaks do not split, because the chiral centre is shifted one carbon away from the binding site and the three ligand arms at the vertices can adopt a symmetric geometry in a less crowded environment. Both ligands form the same assembly in solution, sharing almost identical spectra for complexes 3 and 4. Although it failed to obtain the crystal structures of 3 and 4, the comparable  $^1\text{H}$  NMR spectra of complexes 1–4 in solution imply that ligands  $\text{L}^{1\text{R}}/\text{L}^{1\text{S}}$  and  $\text{L}^{2\text{R}}/\text{L}^{2\text{S}}$  coordinate with phosphate anions to form similar well-defined structures, which cause the similar peak shifts of urea moieties in these ligands. Furthermore, the diffusion coefficients measured by diffusion-ordered NMR spectroscopy (DOSY) experiments for complexes 1 and 3 demonstrated comparable outcomes (Fig. S37, ESI $^\dagger$ ), where a single diffusion coefficient corresponding to the only or dominant species was observed for each complex. The calculated dynamic radii of tetrahedral structures through the Stokes–Einstein equation (12 Å) are in good agreement with the sizes derived from the crystal structures of 1 and 2. Combining the  $^1\text{H}$  NMR and DOSY analysis reveals that similar  $\text{A}_4\text{L}_4$  type anion-tetrahedral cages are formed between ligands  $\text{L}^{2\text{R}}/\text{L}^{2\text{S}}$  and  $(\text{TPA})_3\text{PO}_4$  in solution.

The corresponding mass spectra of complexes 1–5 show the formation of tetrahedrons by ligands and  $\text{PO}_4^{3-}$ . Taking ligand  $\text{L}^{1\text{R}}$  for example, when sprayed from acetonitrile or acetone, a set of mass peaks are found in the spectrum at  $m/z = 1950.7165$  for  $[(\text{PO}_4)_4(\text{L}^{1\text{R}})_4(\text{TPA})_5\text{H}_2]^{3-}$ , 2012.7938 for  $[(\text{PO}_4)_4(\text{L}^{1\text{R}})_4(\text{TPA})_6\text{H}_3]^{3-}$ ,

and 2074.5349 for  $[(\text{PO}_4)_4(\text{L}^{1\text{R}})_4(\text{TPA})_7\text{H}_2]^{3-}$  (Fig. S38, ESI $^\dagger$ ), which are consistent with the simulated patterns. Similar results referring to the  $\text{A}_4\text{L}_4$  cage could also be observed in complexes 2–5 (Fig. S39–S42, ESI $^\dagger$ ).

As mentioned above, it is noted that ligands with predisposed chirality exhibited profound influence on the ultimate chirality of the self-assembled tetrahedral cage. To probe the chirality transfer from an individual ligand molecule to the consequent supramolecular architecture, circular dichroism (CD) measurements were employed. For ligands  $\text{L}^{1\text{R}}$  and  $\text{L}^{1\text{S}}$ , wherein the chiral carbons are directly attached to the urea groups, the CD intensities of the formed complexes are almost the same as that of each other with opposite signals; five peaks at 364, 307, 271, 245, and 231 nm with strong Cotton effects are found in the spectra (Fig. 3, blue and magenta). The crystal structures of the cages provide unambiguous assignment of their stereochemical configuration. The  $\text{L}^{1\text{R}}$  ligand leads to the  $\Delta\Delta\Delta\Delta$  enantiomer, while  $\text{L}^{1\text{S}}$  forms the  $\Lambda\Lambda\Lambda\Lambda$  cage. However, for the ligands ( $\text{L}^{2\text{R}/2\text{S}}$ ) with one more carbon between the chiral center and anion binding site, distinct attenuation of the CD signals (Fig. 3, black and red) can be found at the following wavelengths: 364 (by 99%), 307 (94%), 271 (87%), 245 (89%), and 231 nm (85%). The weak Cotton effects imply that the resulting supramolecular complexes 3 and 4 in solution may be a mixture of diastereomers, with only a slight chirality bias. However, their NMR spectra do not show well-resolved signals of the diastereomers although some peaks are broadened (Fig. S28 and S29, ESI $^\dagger$ ). Based on the CD results, it could be concluded that the position of the introduced chiral site in the ligand is crucial for the chirality transfer. Even a slight difference in the chiral ligands can lead to dramatic differences in the chiral transcription from the individual component to the final supramolecular structures.

To further test the chirality transcription in anion-coordination tetrahedral cages, we introduced the achiral ligand  $\text{L}^{\text{CN}}$  ( $\text{R} = \textit{para}$ -cyanophenyl for  $\text{L}^{\text{CN}}$  in Scheme 1, see details in the ESI $^\dagger$ ) into the cage formed by  $\text{L}^{1\text{S}}$  (or  $\text{L}^{1\text{R}}$ ). Ligand  $\text{L}^{\text{CN}}$ , which was chosen because the most closely related ligand  $\text{L}^{\text{Bn}}$  has a poor solubility, was

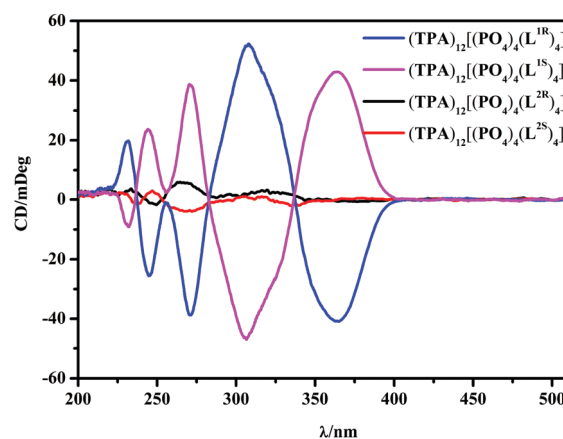


Fig. 3 Circular dichroism spectra of  $(\text{TPA})_{12}[(\text{PO}_4)_4(\text{L}^{1\text{R}/1\text{S}})_4]$  (complexes 1 and 2) and  $(\text{TPA})_{12}[(\text{PO}_4)_4(\text{L}^{2\text{R}/2\text{S}})_4]$  (complexes 3 and 4) in  $\text{CH}_3\text{CN}$ ,  $c = 4 \times 10^{-5} \text{ mol L}^{-1}$  based on ligands.

proved to form the  $A_4L_4$  tetrahedral complex  $(TMA)_{12}[(PO_4)_4(L^{CN})_4]$  (**6**) by NMR and HR-MS (Fig. S32 and S43, ESI<sup>†</sup>). Complex **2** bearing the chiral ligand  $L^{1S}$  was thus mixed with complex **6** in different proportions, 4:0, 3:1, 2:2, 1:3 and 0:4, respectively, in acetonitrile, keeping the total concentration at  $c = 4 \times 10^{-5} \text{ mol L}^{-1}$ . Concentration-dependent  $^1\text{H}$  NMR measurements confirmed the stability of tetrahedral cages at tested concentrations (Fig. S50, ESI<sup>†</sup>). The much more complicated NMR spectra of the mixed solution indicate the ligand exchange process (Fig. S51, ESI<sup>†</sup>), where chiral and achiral ligands are mixed together to build cage structures with concomitant appearance of new peaks in NMR spectra. In the mass spectra, the mixed cages are also found (Fig. S52 and S53, ESI<sup>†</sup>). In the CD spectra (Fig. S49, ESI<sup>†</sup>), upon formation of the mixed-ligand cages when  $L^{1S}$  was mixed with the achiral  $L^{CN}$ , the CD signals gradually weakened, but can still be observed even in the 1:3 ( $L^{1S}$  to  $L^{CN}$ ) system, suggesting the retention of chirality in the chiral-achiral mixed-ligand systems.

In summary, tetrahedral cages formed by ligands ( $L^{1R/1S}$ ) with chiral sites directly linked to the coordination center were enantiopure products, while the chirality of the cages with ligands shifting the point chiral center one carbon away was attenuated to form diastereomers. The results clearly demonstrate the profound influence of prepositioned point chirality in the ligand on the origin of the consequent chirality of the formed structures. Thus, it is evident that the chirality of aniono-supramolecular assemblies, like the metallo-systems, may also be controlled through chiral transcription by introducing chiral auxiliaries into the ligand. Further exploration of the chirality issues in the anion-coordination driven assembly (ACDA) is underway.

We are grateful for the financial support from the National Natural Science Foundation of China (91856102 and 21772154) and Shaan'xi Province (334041900005 and 2019JQ-723).

## Conflicts of interest

There are no conflicts to declare.

## Notes and references

- (a) J. E. Hein and D. G. Blackmond, *Acc. Chem. Res.*, 2012, **45**, 2045–2054; (b) M. Liu, L. Zhang and T. Wang, *Chem. Rev.*, 2015, **115**, 7304–7397; (c) E. M. G. Jamieson, F. Modicom and S. M. Goldup, *Chem. Soc. Rev.*, 2018, **47**, 5266–5311.
- (a) M. Pan, K. Wu, J.-H. Zhang and C.-Y. Su, *Coord. Chem. Rev.*, 2019, **378**, 333–349; (b) D. K. Smith, *Chem. Soc. Rev.*, 2009, **38**, 684–694; (c) O. J. G. M. Goor, S. I. S. Hendrikse, P. Y. W. Dankers and E. W. Meijer, *Chem. Soc. Rev.*, 2017, **46**, 6621–6637; (d) C. Tan, J. Jiao, Z. Li, Y. Liu, X. Han and Y. Cui, *Angew. Chem., Int. Ed.*, 2018, **57**, 2085–2090; (e) L.-J. Chen, H.-B. Yang and M. Shionoya, *Chem. Soc. Rev.*, 2017, **46**, 2555–2576.
- (a) W.-Q. Xu, Y.-Z. Fan, H.-P. Wang, J. Teng, Y.-H. Li, C.-X. Chen, D. Fenske, J.-J. Jiang and C.-Y. Su, *Chem. – Eur. J.*, 2017, **23**, 3542–3547; (b) J. M. Rivera, T. Martín and J. Rebek, *Science*, 1998, **279**, 1021–1023; (c) T. R. Cook and P. J. Stang, *Chem. Rev.*, 2015, **115**, 7001–7045; (d) S. Yoshioka, Y. Inokuma, M. Hoshino, T. Sato and M. Fujita, *Chem. Sci.*, 2015, **6**, 3765–3768; (e) A. M. Castilla, W. J. Ramsay and J. R. Nitschke, *Acc. Chem. Res.*, 2014, **47**, 2063–2073; (f) M. Mastalerz, *Acc. Chem. Res.*, 2018, **51**, 2411–2422; (g) L.-L. Yan, C.-H. Tan, G.-L. Zhang, L.-P. Zhou, J.-C. Bünzli and Q.-F. Sun, *J. Am. Chem. Soc.*, 2015, **137**, 8550–8555; (h) D. S. Kim and J. L. Sessler, *Chem. Soc. Rev.*, 2015, **44**, 532–546.
- (a) S. P. Argent, T. Riis-Johannessen, J. C. Jeffery, L. P. Harding and M. D. Ward, *Chem. Commun.*, 2005, 4647–4649; (b) A. V. Davis, D. Fiedler, M. Ziegler, A. Terpin and K. N. Raymond, *J. Am. Chem. Soc.*, 2007, **129**, 15354–15363; (c) A. M. Castilla, N. Ousaka, R. A. Bilbeisi, E. Valeri, T. K. Ronson and J. R. Nitschke, *J. Am. Chem. Soc.*, 2013, **135**, 17999–18006; (d) C.-T. Yeung, K.-H. Yim, H.-Y. Wong, R. Pal, W.-S. Lo, S.-C. Yan, M. Y.-M. Wong, D. Yufit, D. E. Smiles, L. J. McCormick, S. J. Teat, D. K. Shuh, W.-T. Wong and G.-L. Law, *Nat. Commun.*, 2017, **8**, 1128; (e) C. M. Hong, R. G. Bergman, K. N. Raymond and F. D. Toste, *Acc. Chem. Res.*, 2018, **51**, 2447–2455; (f) Y. Fang, J. A. Powell, E. Li, Q. Wang, Z. Perry, A. Kirchon, X. Yang, Z. Xiao, C. Zhu, L. Zhang, F. Huang and H.-C. Zhou, *Chem. Soc. Rev.*, 2019, **48**, 4707–4730; (g) Z. Wang, L.-P. Zhou, T.-H. Zhao, L.-X. Cai, X.-Q. Guo, P.-F. Duan and Q.-F. Sun, *Inorg. Chem.*, 2018, **57**, 7982–7992; (h) C. Zhao, Q.-F. Sun, W. M. Hart-Cooper, A. G. DiPasquale, F. D. Toste, R. G. Bergman and K. N. Raymond, *J. Am. Chem. Soc.*, 2013, **135**, 18802–18805.
- (a) N. Busschaert, C. Caltagirone, W. Van Rossom and P. A. Gale, *Chem. Rev.*, 2015, **115**, 8038–8155; (b) C. Jia, W. Zuo, D. Yang, Y. Chen, L. Cao, R. Custelcean, J. Hostaš, P. Hobza, R. Glaser, Y.-Y. Wang, X.-J. Yang and B. Wu, *Nat. Commun.*, 2017, **8**, 938; (c) D. Yang, J. Zhao, X.-J. Yang and B. Wu, *Org. Chem. Front.*, 2018, **5**, 662–690; (d) X. Bai, C. Jia, Y. Zhao, D. Yang, S. C. Wang, A. Li, Y.-T. Chan, Y.-Y. Wang, X.-J. Yang and B. Wu, *Angew. Chem., Int. Ed.*, 2018, **57**, 1851–1855; (e) K. Bowman-James, *Acc. Chem. Res.*, 2005, **38**, 671–678.
- B. Wu, F. Cui, Y. Lei, S. Li, N. D. S. Amadeu, C. Janiak, Y. J. Lin, L. H. Weng, Y. Y. Wang and X.-J. Yang, *Angew. Chem., Int. Ed.*, 2013, **52**, 5096–5100.
- (a) D. Yang, J. Zhao, Y. Zhao, Y. Lei, L. Cao, X.-J. Yang, M. Davi, N. D. S. Amadeu, C. Janiak, Z. Zhang, Y. Y. Wang and B. Wu, *Angew. Chem., Int. Ed.*, 2015, **54**, 8658–8661; (b) D. Yang, J. Zhao, L. Yu, X. Lin, W. Zhang, H. Ma, A. Gogoll, Z. Zhang, Y. Wang, X.-J. Yang and B. Wu, *J. Am. Chem. Soc.*, 2017, **139**, 5946–5951; (c) W. Zhang, D. Yang, J. Zhao, L. Hou, J. L. Sessler, X.-J. Yang and B. Wu, *J. Am. Chem. Soc.*, 2018, **140**, 5248–5256.
- W. Zuo, Z. Huang, Y. Zhao, W. Xu, Z. Liu, X.-J. Yang, C. Jia and B. Wu, *Chem. Commun.*, 2018, **54**, 7378–7381.
- (a) M. Wei, B. Wu, L. Zhao, H. Zhang, S. Li, Y. Zhao and X.-J. Yang, *Org. Biomol. Chem.*, 2012, **10**, 8758–8761; (b) B. Li, B. Zheng, W. Zhang, D. Zhang, X.-J. Yang and B. Wu, *Cryst. Growth Des.*, 2019, **19**, 6527–6533.